Bollettino di Geofisica Teorica ed Applicata Vol. 62, n. 1, pp. 89-100; March 2021
DOI 10.4430/bgta0331

Integrating the pre-stack seismic data inversion and seismic attributes to estimate the porosity of Asmari Formation

A. Jelvegar Filband[1] and M.A. Riahi[2]

[1] *Department of Physics, Islamic Azad University, Central Branch, Tehran, Iran*
[2] *Institute of Geophysics, University of Tehran, Iran*

(Received: 14 February 2020; accepted: 12 May 2020)

ABSTRACT In this study, the inversion of seismic data has been used in integration with the seismic attributes in order to evaluate the reservoir porosity in the Ghar member of the Asmari Formation for an oil field located in SW Iran. Using the inversion method based on acoustic impedance modelling, the compressional wave velocity and density are extracted and, then, the linear and nonlinear conversion between the seismic attributes and the porosity log is used to obtain the optimum porosity volume for the region. In this study, we have used pre-stack seismic data to estimate reservoir porosity. The combination of selected seismic attributes along with the raw seismic data is used to estimate the porosity by the neural network method. In order to validate the utilised method, the cross-validation technique has been used to compare the accuracy of the calculated petrophysical parameters with the actual values. The correlation coefficient obtained for the estimated porosity is 81%. This value indicates that the training data were appropriate, optimally estimating the actual porosity using the selected attributes.

Key words: seismic attributes, porosity, neural network, Asmari Formation.

1. Introduction

Hydrocarbon reservoirs are one of the most important energy resources for mankind today, therefore, using more efficient and less costly methods for developing hydrocarbon reservoirs is inevitable. In exploration and production activities, a quantitative description of reservoir properties, using all available petrophysical, seismic, and geological data, can play a significant role in the development of oil fields and enhanced recovery of the reservoir (Pendral, 2001; Çemen *et al*., 2014). In recent years, the use of seismic inversion to estimate reservoir properties has been a useful tool in the oil and gas industry (Alsos *et al*., 2018; Ghanbarnejad Moghanloo *et al*., 2018; Qiang *et al*., 2020). Seismic inversion is a method of extracting the subsurface properties using seismic data as input (Doyen, 1988; Russell and Hampson, 1991). The main purpose of seismic inversion is to convert seismic data into quantitative rock properties (White, 1991; Dolberg *et al*., 2000). In the model-based inversion used in this study, by building an initial geological model and estimating the seismic wavelet, the acoustic impedance of the Earth layers is extracted from seismic data. Acoustic impedance data are used for quantitative characterisation of reservoir properties for reservoir modelling (Ling, 2003; Russell *et al*., 2003). Seismic attributes are extracted from seismic data in the time and frequency domains. Attributes derived from time variables include

structural information and domain-derived attributes include stratigraphic information. Frequency attributes contain information about reservoir properties (Li and Zhao, 2014). Seismic attributes are extracted from pre-stack and post-stack seismic data. Post-stack seismic attributes can be extracted on a time slice or between two horizons (Brown, 2001). Compared to seismic amplitudes, the results of inversion have higher resolution and convey more accurate interpretations (Pendrel, 2006; Li and Zhao, 2014). Post-stack inversion is the process of calculating the final impedance model of the subsurface using post-stack seismic data which, in turn, determines the geology of the subsurface (Hampson-Russell, 2007; Xinyang *et al*., 2015). The purpose of this research is to determine the reservoir characteristics using seismic data inversion methods and the integration of seismic attributes in one of the carbonate reservoir oil fields located SW of Iran.

2. Geological setting

The Zagros-Persian Gulf region is part of the giant sedimentary basin of Iran, Saudi Arabia, and Iraq, which is the world's largest oil-bearing sedimentary basin (Ghazban, 2007). The Ghar Formation can be correlated with the older (Oligocene) Ahwaz sandstone Member of the Asmari Formation in the SW of Iran (James and Wynd, 1965; Powers *et al*., 1966). In this study, the Asmari Formation and the Ahwaz sandstone Section (Ghar Formation) were studied in a field located NW of the Persian Gulf, 100 km SW of the Kharg Island (Ghazban, 2007). In the study area, the Asmari Formation is divided into two upper and lower reservoir layers and the Ghar Formation is located in the middle. In this oilfield, the Upper Asmari Formation lithology consists of anhydrite, dolomite, calcite, and illite. The Ghar Formation mostly consists of sandstone and smaller quantities of dolomite, calcite, and illite. The Lower Asmari Formation includes carbonate lithology and small amount of illite and calcite (Aghanabati, 2004; Ghazban, 2007).

3. Method

The data required in this study include three-dimensional seismic data, petrophysical logs as well as geological data from the region. To do this research, the Hampson-Russell (2007) software was used to perform the seismic inversion, and the extraction of seismic attributes was performed using the commercial Petrel software. Fig. 1 shows the workflow performed in this study.

In this study, we used the pre-stack time-migrated seismic data with a sampling rate of 4 ms in the SEGY format and employed related well logs from the oil field. The first step in pre-stack inversion is to load seismic data, well logs, headers, check shots on well logs, as well as the interpreted seismic horizons. Determining the top and base reservoir reflectors is also an important geological application for matching seismic and well information. Fig. 2 shows the pre-stack seismic data loaded with interpreted horizons in this interval.

Well logs have been loaded into the software. The logs from the A-10 well include gamma ray, sonic wave velocities, and density. In addition to the above logs, shear wave velocity is also recorded for well A-17 (Fig. 3).

The model-based inversion method requires that a seismic wavelet has to be introduced to calculate a synthetic seismic trace. A synthetic seismic trace will be calculated based on the

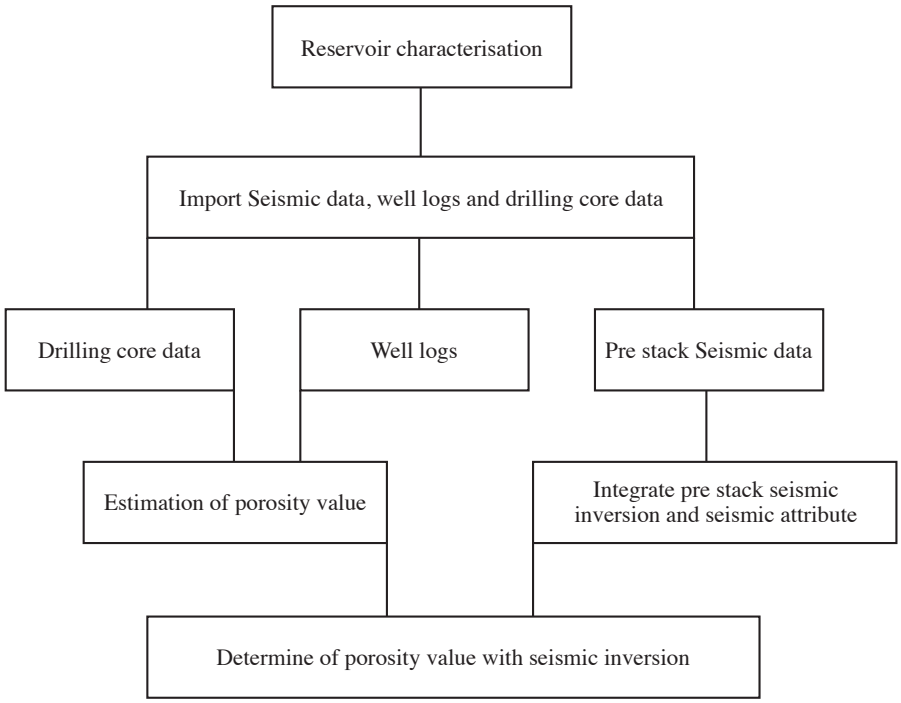

Fig. 1 - Workflow applied in this study.

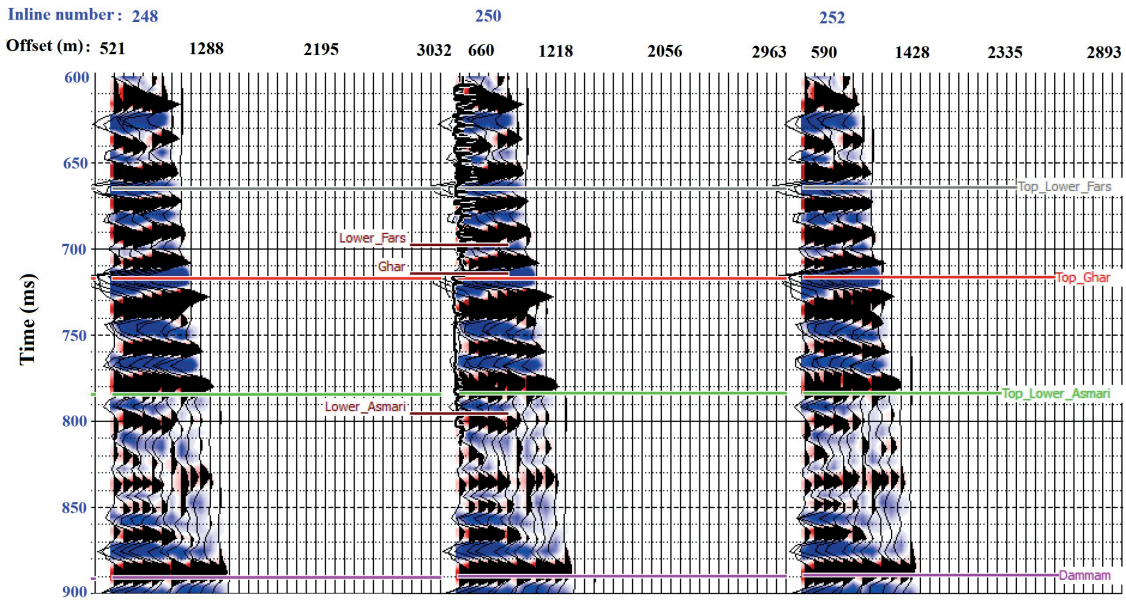

Fig. 2 - Seismic data and interpreted horizons of the investigated field.

convolution between initial estimated acoustic impedance and the introduced wavelet. The acoustic impedance is, then, corrected and adjusted using check shot. In this approach, after estimating the series of reflection coefficients from the sonic log recorded at well site, different seismic wavelets are extracted (Yi *et al*., 2013; Rahimi and Riah, 2020). In the spectral division

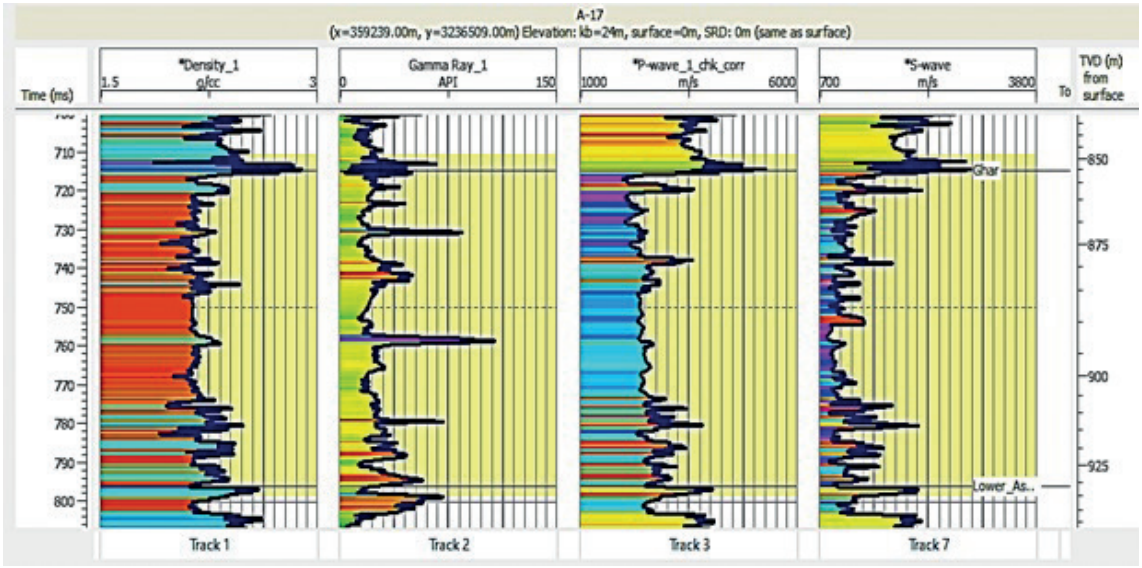

Fig. 3 - Logs recorded at the well A-17.

method, seismic mapping in the frequency domain is the product of the Fourier transform of the reflection coefficient series and the Fourier transform of the wavelet. As the Fourier transform of seismic mapping at the well is divided by the Fourier transform of the reflection coefficients of the well logs, the constructor wavelet is obtained. At places where the reflection coefficients are equal to zero, the Fourier transform is the series of zero reflection coefficients and, hence, there is the problem of dividing by zero. The wavelets are extracted using three seismic angle gather data ranging from 0° to 10° as the near offset, 11° to 20° as the middle offset, and 21° to 29° as the far offset (Fig. 4). The wavelets are 140 ms long and the phase of all three wavelets is equal to zero degrees. As shown in Fig. 4, the seismic data has a wide frequency spectrum, which improves the quality of the results.

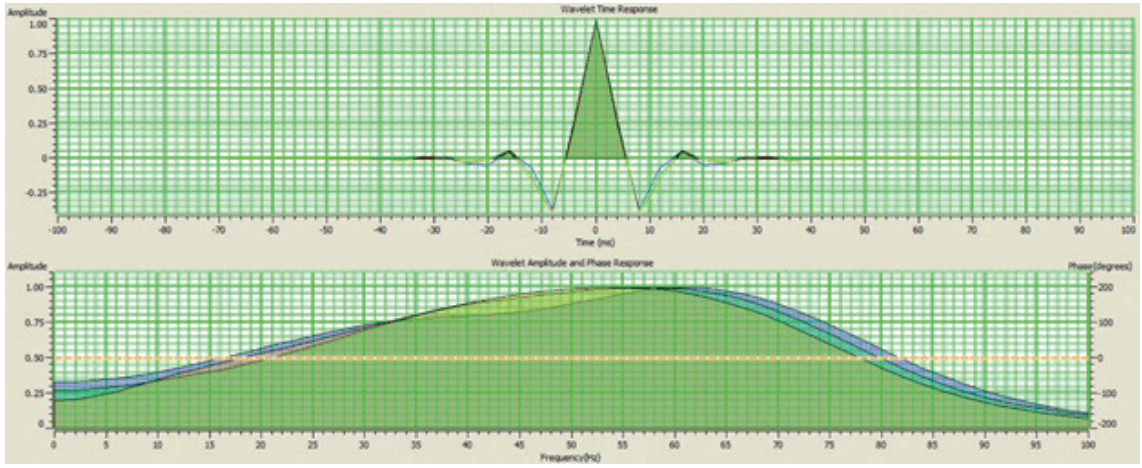

Fig. 4 - Simultaneous representation of three angle-dependent wavelets extracted statistically.

After the inversion, the sections of compressional acoustic impedance, shear impedance, and the density are obtained. Figs. 5 and 6 show a cross-section of the volume obtained from acoustic impedance. As it can be seen in Fig. 5, the amount of acoustic impedance in the interval of interest (reservoir interval) is reduced towards the top and the base layers which indicates the high porosity of the reservoir layer.

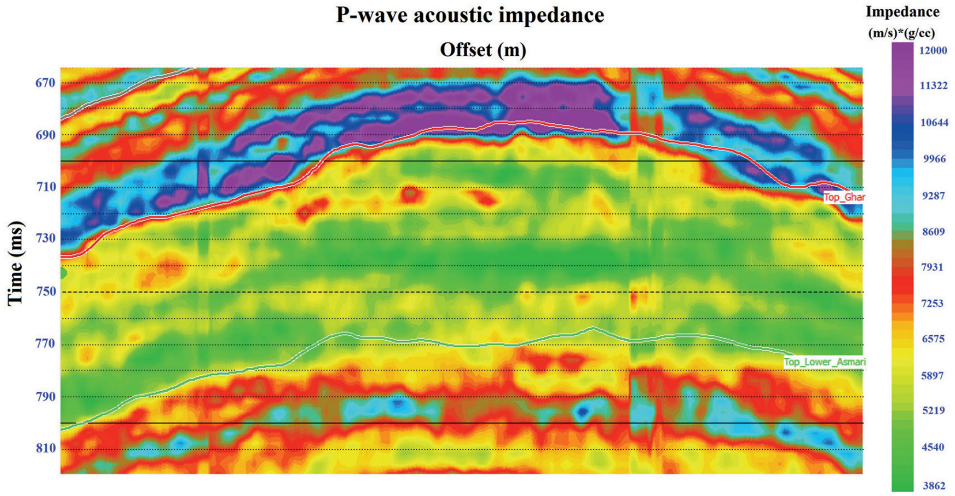

Fig. 5 - The cross-section of the P-wave acoustic impedance resulting from pre-stack elastic seismic inversion.

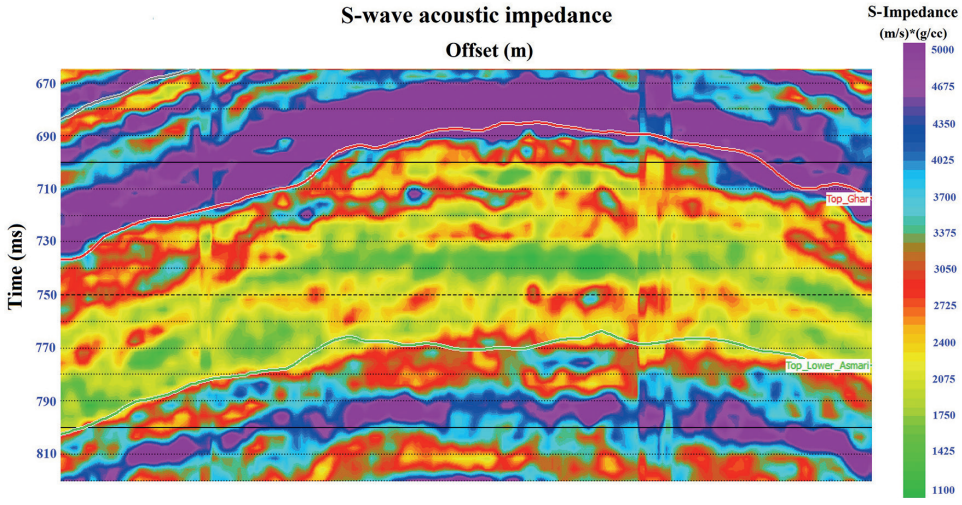

Fig. 6 - The cross-section of the S-wave acoustic impedance resulting from pre-stack elastic seismic inversion.

In Fig. 7 we also see that the density cross-section in the reservoir interval is slightly lower than the top and base layers.

3.1. Probabilistic neural network (PNN)

The Probabilistic Neural Network (PNN) is an intelligence neural network, which is frequently used in classification and pattern recognition problems. The estimation of petrophysical property model from well log data is mainly performed via empirical, statistical, and intelligent systems

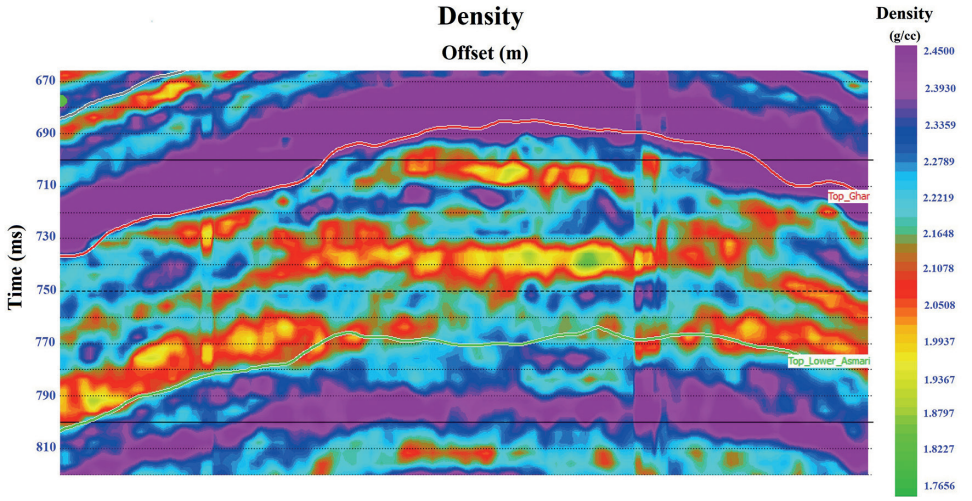

Fig. 7 - Density cross-section resulting from pre-stack elastic seismic inversion.

methods. The empirical technique is based on core measurements to develop mathematical models. PNN is an alternative type of neural network using a mathematical interpolation (Specht, 1990; Masters, 1995). PNN assumes that each new log output can be written as a linear combination of log values in the training data. PNN can be written using equations:

$$\begin{aligned} &\{A11, A21, A31, L1\} \\ &\{A12, A22, A32, L2\} \\ &\{A13, A23, A33, L3\} \\ &\quad \ldots \\ &\{A1n, A2n, A3n, Ln\} \end{aligned} \tag{1}$$

where n is training data, and there are three attributes to be used. Li is the target log that will be predicted. PNN assumes that each value of the output log can be written as a linear combination of the input log values. The new data sample with corresponding attribute values can be written as:

$$x = \{A1j, A2j, A3j \ldots Anj\} \tag{2}$$

Then, the new log quantity will be calculated using the following equation:

$$l(x) = \frac{\sum_{i=1}^{n} Li * \exp(-D(x, xi))}{\sum_{i=1}^{n} \exp(-D(x, xi))} \tag{3}$$

where

$$D(x, xi) = \sum_{j=1}^{3} \left(\frac{xj - xij}{\delta j} \right). \tag{4}$$

The quantity $D(x, xi)$ is the 'distance' between the input point and each of the training points xi. This D is measured in the multi-dimensional space spanned by the attributes, and it is scaled by the quantity $j\sigma$, which may be different for each of the attributes:

$$E(\sigma 1,\sigma 2,\sigma 3) = \sum_{i=1}^{n} (Li - \hat{L}i) \wedge 2 \, . \tag{5}$$

Note that the prediction error depends on the choice of the parameters, σj. This quantity is minimised using a nonlinear conjugate gradient algorithm described in Masters (1995). The results obtained by PNN analysis will form a nonlinear transformation between the target log and the seismic attributes in the cross-plot diagram. The results of non-linear transformations expect a better correlation value between the actual log and the log model compared to the results of linear transformations generated through a decrease in multi-attributes.

4. Porosity estimation using seismic attributes

Since seismic inversion is one of the tools for extracting useful information from seismic data, innovating new techniques in this area have been steadily increasing in recent years. As the next step to our workflow, the neural network capabilities of the Emerge module in the Hampson-Russell (2007) software are used for porosity estimation. This module utilises a variety of PNN such as statistical neural networks, normal discriminant analysis (NDA), neural networks with radial basis functions, and leading neural networks for such purpose. PNNs are useful in quantifying reservoir properties due to their ability to solve complex and functional equations efficiently finding reservoir properties (Specht, 1990; Masters, 1995). This network is a variety of radial networks and their performance is similar to that of radial networks. The PNN consists of two layers similar to other neural networks. The second layer in this network, unlike other neural networks, is competitive and target outputs must be entered in the form of index vectors with values of 0 and 1. Similarly for other inputs, this operation is repeated. Finally, the sum of the computed intervals in the form of a probabilistic vector is passed to the output layer and the values are obtained through functions related to the network output values.

In order to estimate the porosity using seismic attributes, 28 different attributes were investigated. The correlation coefficient of all these 28 attributes with porosity was calculated. The attributes that had the highest correlation coefficient with porosity were selected. Then, to increase the accuracy of the estimation, attribute group information was used to estimate the porosity (Table 1).

In other words, several attributes were used simultaneously to increase the accuracy of porosity estimation at the well site (Fig. 8).

An important point is to determine the proper number of attributes. The black curve in Fig. 8 shows the training error, the vertical axis the mean error, and the horizontal axis the number of attributes. Mathematically, the training-error curve should always be descending. There is always the principle that increasing the attributes will better predict the target parameter. However, this does not mean that the added attributes predict the correct signal of the target parameter, but it may predict the noise in the target parameter as well. Increasing attributes are like fitting higher-order polynomials to a set of points. We need a benchmark to figure out where to stop adding new attributes.

Table 1 - Training error and final attribute validation error.

Parameter	Seismic attribute	Training error	Validation error
porosity	Z_p^2	0.053	0.084
porosity	Z_s^2	0.050	0.082
porosity	Instantaneous frequency	0.047	0.079
porosity	Instantaneous amplitude	0.045	0.076
porosity	Instantaneous cosine phase	0.043	0.072
porosity	Instantaneous phase	0.042	0.070
porosity	Apparent polarization	0.041	0.092

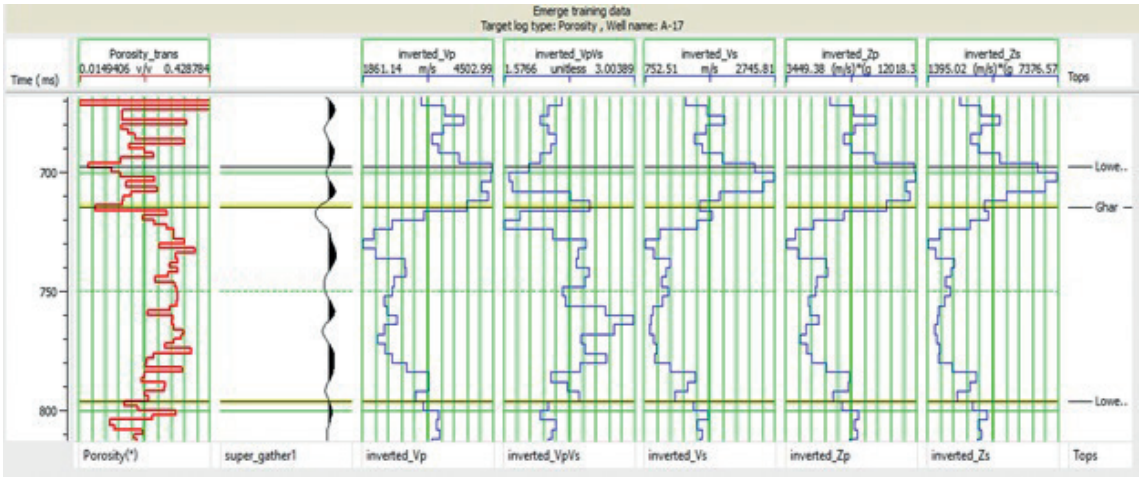

Fig. 8 - Five attributes used in the training phase at Well 17 in the Ghar member reservoir interval down to the Asmari Formation.

Each point in the validation error is estimated using the technique of disregarding one well and predicting its values using the operator calculated with the other wells. For example, the last red dot corresponding to the seven attributes is calculated as follows: the seven attributes listed are sorted in Table 1. First, Well 1 is excluded from the calculation. The weight of seven attributes is calculated for the rest of the wells. The obtained operator is, then, used to predict the values in Well 1. Since we already know the exact values, the RMS error is stored for Well 1. Then, Well 2 is ignored and the whole process is repeated. The last point in the validation curve is the mean error, which is calculated for all wells. This indicates an error that can be expected if a new well is added. For this reason, the validation curve is a good measure of the validation of the analysis.

As it is clear from the validation error, using the first six attributes, the validation error is reduced. But with the addition of the seventh attribute, the validation error increases. From this curve, it can be seen that no more than the first six properties are used to calculate porosity, since for the seventh attribute no reduction in validation error takes place. In fact, adding the seventh attribute will cause more error and reduces the prediction accuracy. Therefore, the six primary attributes are selected to estimate the porosity parameter. Each point in the validation error is estimated using the technique of excluding one well and predicting its values using the operator calculated by including other wells. For example, the last red dot corresponding to the seven

attributes is calculated as follows: the seven attributes listed are sorted in the Table 1. To perform this step, Well 1 is excluded from the calculation process.

The red curve in Fig. 9 illustrates the validation error, and this curve can guide us in deciding how many attributes to use.

Fig. 10 shows the predicted porosity using data training against actual porosity at the well locations. The correlation coefficient was 81% indicating that the training data were appropriate and this method was able to estimate the actual porosity using the listed attributes (Table 1).

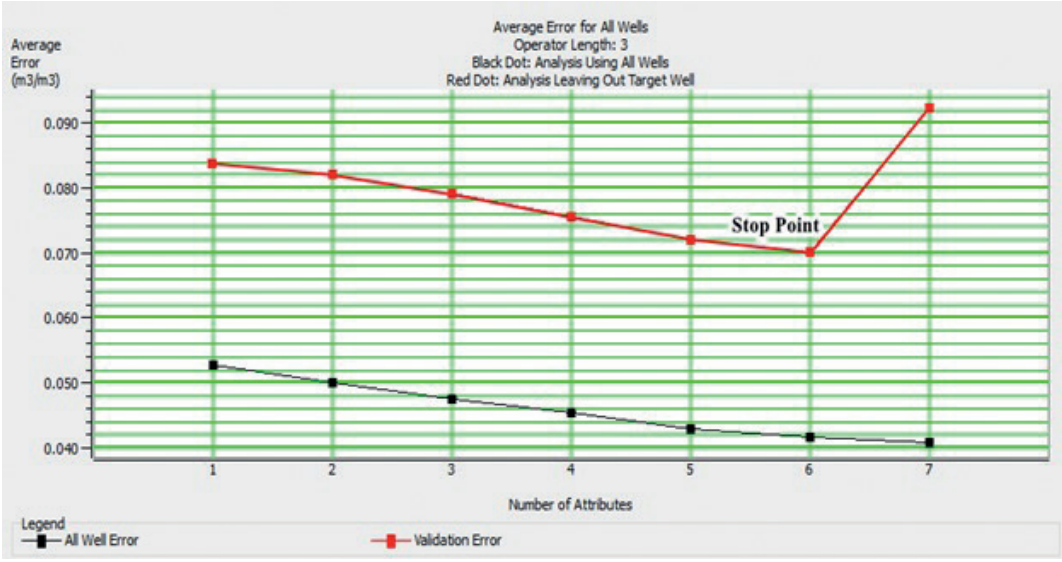

Fig. 9 - Validation error and prediction error in all wells in the reservoir interval. The first six attributes demonstrate least prediction error.

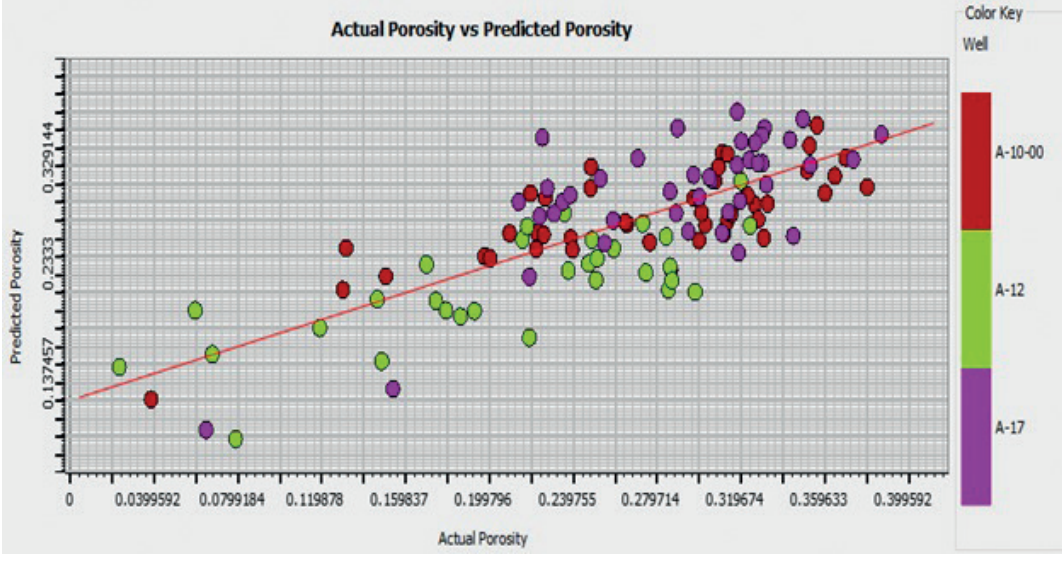

Fig. 10 - Predicted porosity using data training versus actual porosity in wells. The correlation coefficient was 81% and error was 3.6%.

Now, we have obtained a relation between porosity and a set of seismic attributes. The obtained relationship is now applied to the whole seismic data volumes. Fig. 11 is a section of the porosity parameter in the reservoir interval. As it is shown, the porosity at the top the reservoir is lower (about 23%); within the Ghar member, porosity increases (about 28%). Overall, it can be said that the porosity of the Ghar member is considerable, due to its sandy composition (Aghanabati, 2004; Alizadeh *et al*., 2008).

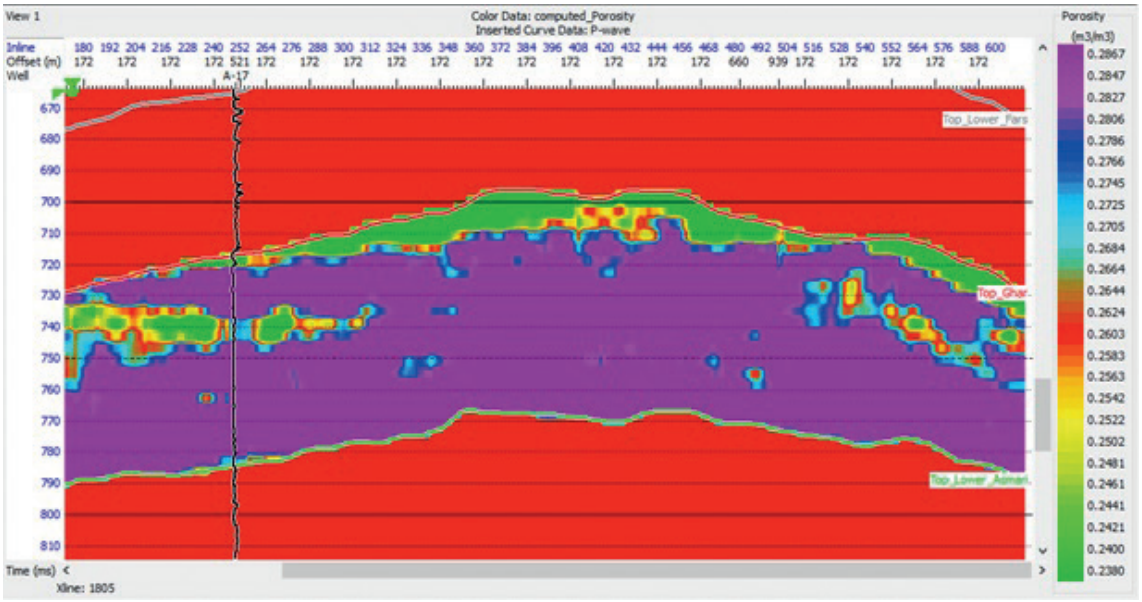

Fig. 11 - Porosity section calculated at the reservoir interval. The upper layer of the Ghar member has less porosity and it increases in porosity within the Ghar member.

Fig. 12 shows a time slice at 730 ms of porosity distribution in the reservoir interval (a time window of 20 ms above and below the Ghar member's horizon). As it can be seen in the figure, the high porosity segments are well separated from the low porosity segments. These ranges can be considered for infill drilling.

5. Verification

In this study, in order to validate the utilised methodology, a well was excluded from the relevant calculations to compare the accuracy of the calculated petrophysical parameters with the actual values. Table 2 shows the comparison between estimated parameters with actual petrophysical values at the well location. The results show that the proposed methodology provides a good estimation of the desired parameters with reasonable accuracy.

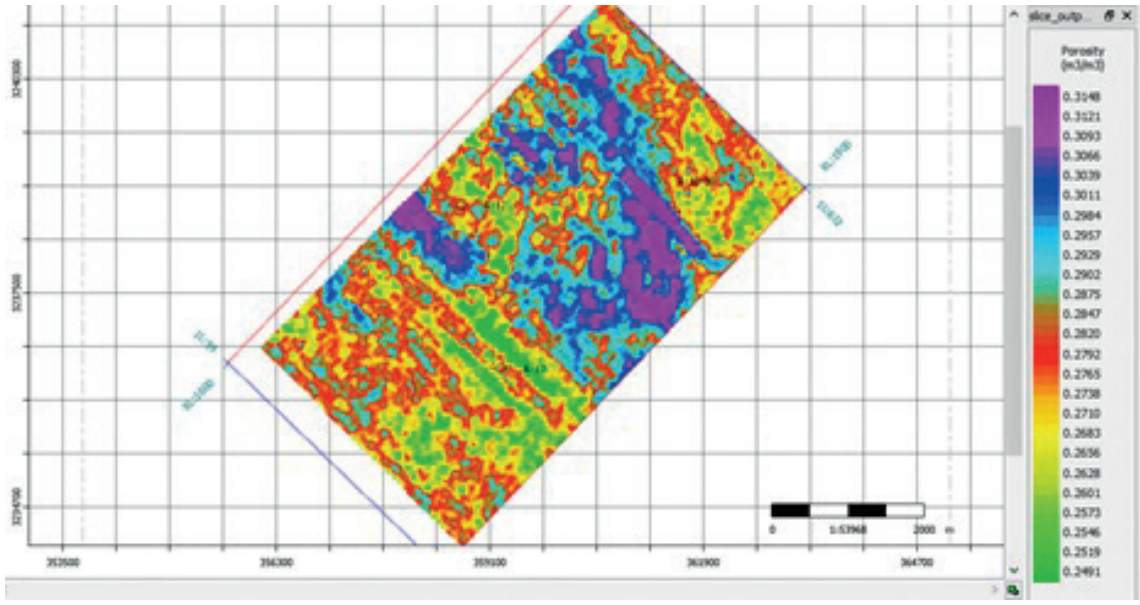

Fig. 12 - Time slice at 730 ms of porosity distribution in the reservoir interval. Areas with high porosity (purple colour) are well separated from other areas.

Table 2 - Comparison between the porosity calculated using the well log of a test well with the estimated porosity.

Time (MS)	Estimated porosity (%)	Porosity value of well test (%)
718	20.12	19.98
724	43.35	40.31
750	32.12	32.78
772	30.95	31.90
790	29.41	30.83

6. Conclusions

In this study, compressional acoustic impedance, shear impedance, and density were obtained using pre-stack elastic seismic inversion of the seismic data. These parameters in the reservoir interval showed significant reduction. The use of elastic inversion in this study enabled the estimation of shear wave in addition to compressional wave velocity in the seismic data. In addition, the ratio of the compressional wave to the shear wave was calculated. All of these attributes were used in the data training phase. Therefore, the presence of shear wave information and shear wave impedance as independent external attributes helped to increase the accuracy of petrophysical parameter estimation. The time slice of the porosity distribution corresponding to the Ghar member revealed a hydrocarbon zone east of the oil field and two oil-bearing channels located SW of the field. These areas can be designated as proposed drilling locations for field development. The correlation coefficient obtained for porosity estimation is 81%. This value indicates that the training data is appropriate, and can estimate the actual porosity to the desired extent using the proper attributes.

Acknowledgements. The second author acknowledges the research council of the University of Tehran. We acknowledge the journal, two anonymous reviewers, for their insightful comments. This research did not receive any specific grant from funding agencies.

REFERENCES

Aghanabati A.; 2004: *Geology of Iran, 1st ed*. Ministry of Industry and Mines, Geological Survey of Iran, Tehran, Iran, 582 pp.

Alizadeh M., Bargrizan M. and Yazdanian J.; 2008: *Study and petrophysical evaluation of Ghar horizon from Asmari Formation in Hendijan field located in the Persian Gulf*. Presented at the 12th Symposium of the Geological Society of Iran, Ahvaz, Iran.

Alsos T., Pickering S., Schultz G., Livingstone M. and Nickel M.; 2018: *Seismic applications throughout the life of the reservoir*. Oilfield Review Summer 2002, pp. 48-65.

Brown A.R.; 2001: *Understanding seismic attributes*. J. Geophys., **66**, 47-48.

Çemen I., Fuchs J., Coffey B., Gertson R. and Hager C.; 2014: *Correlating porosity with acoustic impedance in sandstone gas reservoirs: examples from the Atokan sandstones of the Arkoma Basin, southeastern Oklahoma*. In: Proc., Annual Convention Exhibition, Search and Discovery, American Association Petroleum Geologists, Pittsburgh, PA, USA, Article #41255, <http://www.searchanddiscovery.com/documents/2014/41255cemen/ndx_cemen.pdf>, accessed 3 May 2017.

Dolberg D.M., Helgesen J., Hanssen T.H., Magnus I., Saigal G. and Pedersen B.K.; 2000: *Porosity prediction from seismic inversion, Lavrans field, Halten terrace, Norway*. The Leading Edge, **19**, 392-399, doi: 10.1190/1.1438618.

Doyen P.M.; 1988: *Porosity from seismic data: a geostatistical approach*. J. Geophys, **53**, 1263-1275.

Ghanbarnejad Moghanloo H., Riahi M.A. and Bagheri M.; 2018: *Application of simultaneous prestack inversion in reservoir facies identification*. J. Geophys. Eng., **15**, 1376-1388, doi: 10.1088/1742-2140/aab249.

Ghazban F.; 2007: *Petroleum geology of the Persian Gulf*. Tehran University and National Iranian Oil Company Publications, Tehran, Iran, 707 pp.

Hampson-Russell; 2007: *Strata Guide 2007*. Compagnie Générale de Geophysique (CGG) of Veritas DGC Inc., Houston, TX, USA, 89 pp.

James G.A. and Wynd J.G.; 1965: *Stratigraphic nomenclature of Iranian oil consortium agreement area*. Am. Assoc. Pet. Geol. Bull., **49**, 2182-2245.

Li M. and Zhao Y.; 2014: *Prestack seismic inversion and seismic attribute analysis*. In: Geophysical Exploration Technology, Applications in Lithological and Stratigraphic Reservoirs, Elsevier Inc., Amsterdam, The Netherlands, Chapter 7, pp. 199-219, doi: 10.1016/B978- 0-12-410436-5.00007-1.

Ling Y.; 2003: *Study on application of basic seismic attributes to interpretation of depositional environment*. Oil Geophys. Prospect., **38**, 642-653.

Masters T.; 1995: *Advanced algorithms for neural networks*. John Wiley & Sons Inc., New York, NY, USA, 448 pp.

Pendrel J.; 2001: *Seismic inversion - The best tool for reservoir characterization*. Can. Soc. Explor. Geophys. Rec., **26**, 18-24.

Pendrel J.; 2006: *Seismic inversion - A critical tool in reservoir characterization*. Scand. Oil-Gas Mag., **5**, 19-22.

Powers R.W., Ramirez L.F., Redmond C.D. and Elberg E.L.; 1966: *Sedimentary geology of Saudi Arabia*. In: The Geology of the Arabian Peninsula, USGS, Washington, DC, USA, Prof. Paper 560-D, 177 pp.

Qiang Z., Yasin Q., Golsanami N. and Du Q.; 2020: *Prediction of reservoir quality from log-core and seismic inversion analysis with an artificial neural network: a case study from the Sawan gas field, Pakistan*. Energies, **13**, 486-504, doi: 10.3390/en13020486.

Rahimi M. and Riahi M.A.; 2020: *Static reservoir modeling using geostatistics method: a case study of the Sarvak Formation in an offshore oilfield*. Carbonates Evaporites, **35**, 62, doi: 10.1007/s13146-020-00598-1.

Russell B. and Hampson D.; 1991: *A comparison of post-stack seismic inversion methods*. In: Expanded Abstracts, 61st Annual International Meeting, Society of Exploration Geophysicists, Houston, TX, USA, pp. 876-878.

Russell B.H., Hedlin K., Hilterman F.J. and Lines L.R.; 2003: *Fluid-property discrimination with AVO: a Biot-Gassmann perspective*. J. Geophys., **68**, 29-39, doi: 10.1190/1.1543192.

Specht D.F.; 1990: *Probabilistic neural network*. Neural Networks, **3**, 109-118, doi: 10.1016/0893-6080(90)90049-Q.

White R.E.; 1991: *Properties of instantaneous seismic attributes*. The Leading Edge, **10**, 26-32, doi: 10.1190/1.

Xinyang D., Jiyu L., Yuchao C. and Fan L.; 2015: *A study on seismic inversion method for identification of sand*. IOSR J. Eng., **5**, 38-43.

Yi B.Y., Lee G.H., Kim H-J., Jou H-T., Yoo D.G., Ryu B.J. and Lee K.; 2013: *Comparison of wavelet estimation methods*. Geosci. J., **17**, 55-63, doi: 10.1007/s12303-013-0008-0.

Corresponding author: M.A. Riahi
Institute of Geophysics, University of Tehran
North Kargar Ave., Tehran, Iran
Phone: +98 216 1118219; e-mail: mariahi@ut.ac.ir